전 용 필 교수지도

석사학위 청구논문

Controlled Hippo signaling pathway in AMH (anti-Müllerian hormone) mediated folliculogenesis

2022

성신여자대학교 일반대학원

생물학과

김 주 은

Controlled Hippo signaling pathway in AMH (anti-Müllerian hormone) mediated folliculogenesis

Adviser: Yong-Pil Cheon, Ph.D.

Submitted in partical fulfillment
of the requirements for the degree of master.

Nov, 2021

Department of Biology

The Graduate School of Sungshin University

Ju Eun Kim

Certificate of Committee Approval

Be accepted partial fulfillment
of the requirements for the degree of
: Master of Science

Signatures:

Committee Chairman .....
Sung Ho, Lee, Ph. D.

Committee Member Donghyun Lim .....
Dong Hyun Lim, Ph.D.

Committee Member .....
Yong-Pil Cheon, Ph.D.

The Graduate School of Sungshin University

ABSTRACT

Controlled Hippo signaling pathway in AMH (anti-Müllerian hormone) mediated Folliculogenesis

Ju Eun Kim
Department of Biology
Graduate School
Sungshin University

Müllerian inhibiting substance (MIS) known as Anti-Müllerian hormone (AMH) is a critical factor for sex differentiation during embryogenesis and for follicle recruitment in ovary. MIS inhibits follicle stimulating hormone (FSH) dependent follicle growth by reducing sensitivity to FSH and the recruitment of primordial follicle to primary follicle. On the other hand, primordial follicle activation is observed in ovarian tissue piece along with Hippo signaling activation that is known as one of the organ size regulating factors. Hippo signaling pathway is essential for maintaining optimal organ size and consist of several negative growth regulators acting on the kinase cascade. When the Hippo pathway is activated, mammalian Ste-20 like kinase (MST) 1/2 phosphorylate large tumor suppressor kinase (LATS) 1/2. LATS1/2 inactivates Yes-associated protein (YAP) and WW domain containing transcription regulator 1 (WWTR1, also known as TAZ) by phosphorylation. When the Hippo pathway is inactivated, the

dephosphorylated YAP/TAZ translocates into the nucleus and promotes cell proliferation, survival, and self-renewal by binding to TEA-binding domain family member 1 (TEAD) to increase target gene transcription. Transient activation of YAP1 in ovaries can promote follicular growth, and it has been found that LATS1 plays a role in maintaining the primordial follicle pool. In vitro ovarian fragmentation inactivated Hippo signaling, leading to nuclear translocation of YAP, and increased expression of the YAP target gene, which promotes granulosa cell proliferation and inhibits apoptosis. Even though, both of AMH and Hippo pathway are involved in follicle activation and growth, so far, the evidence for interaction between AMH and Hippo is poor. In this study, the relationship of AMH and Hippo in folliculogenesis was evaluated using ovarian cutting model and *Amh* knockout model. The expression profiles of YAP, expression of *Ctgf, Areg, Id1,* and *Ddit4* as evaluated and histological analysis. The weight of ovary after cutting was increased in time-dependent manners in both wild and *Amh* null mice. In *Amh* null ovary, the increase of their weight were slower than that of wild. There was a significant increase in the expression of YAP/TAZ after ovarian partial resection in mice, but the level was lower in Amh KO ovary than in the wild type. At the same time, the number of secondary and tertiary follicles were significantly increased in partially resected ovary with increased expression level of Hippo signaling pathway components. Though further studies are needed, these results suggest that AMH may be related with the expression of Hippo signal transduction mediators.

CONTENTS

List of Tables

List of Figures

INTRODUCTION

Ovarian volume showed a strong correlation with follicular density and folliculogenesis (Lass et al., 1997) because the follicle is a main ovarian construct. In most mammals, no new oocytes are produced after birth, and the follicles presented at birth serves as a reservoir for all oocytes used throughout the female reproductive lifespan. The size of this initial pool of primordial follicles in part determines the reproductive lifespan of the female (Dunlop et al., 2014). After puberty, the primordial follicles undergo folliculogenesis to mature and ovulate oocytes (Fig. 1). In humans and mice, the size of the ovaries gradually increases after birth, and decreases in older females when fertility begins to decline (Lliberos et al., 2021). Ovarian folliculogenesis in mammals is a cyclic and dynamic process that involves dramatic change in the size and number of various cell types of the ovary (Stephanie et al., 2015). One of the many important factors involved in this process is anti-Müllerian hormone (AMH).

In ovary, AMH is a glycoprotein expressed in granulosa cells of small growing ovarian follicles (Gruijters et al., 2003). It belongs to the transforming growth factor β (TGF-β) super family, and this family member plays an variouse roles in mesenchymal–epithelial interaction, cell growth, extracellular matrix (ECM) production, and tissue remodeling. Two types of SMAD proteins are involved in TGF-β signaling, receptor-regulated Smad (R-Smad; Smad1, Smad2, Smad3, Smad5 and Smad8/9) and common Smad (Co-smad; Smad4), and two serine/threonine kinase receptors called type Ⅰ and type Ⅱ. AMH works through its specific receptors. AMH type Ⅱ receptors are specific, but the identity of AMH type Ⅰ receptors is not clearly known (di Clemente et al., 2003).

AMH binds to the AMHRⅡ receptor, to form the AMHRⅡ-ALK2, 3 and 6 transmembrane serine/threonine kinase complex. And activates R-Smad1, 5 and 8 through phosphorylation.

Previously, the role of AMH in male sex differentiation is well known. AMH prevents Müllerian ducts from developing into uterus and other Müllerian structures. During male fetal sex differentiation, AMH is synthesized by testicular sertoli cells and induces the degeneration of Müllerian ducts that form the uterus, fallopian tubes, and upper vagina (Münsterberg et al., 1991). In *Amh* null male mice, the reproductive organs make female reproductive organs and they are often sterile.

During female fetal sex differentiation AMH is not expressed in the ovary. AMH is first expressed in the granulosa cells of the recruited primary follicles that are found in mouse ovaries on postnatal day 3, and in the human fetus after 36 weeks of gestation (Visser et al., 2005). AMH inhibits the development of primordial follicles in the early stages of ovarian follicular development (Sacchi et al., 2016) and plays an important role in folliculogenesis (Hayes et al., 2016). The *Amh* knockout (KO) mice demonstrated that AMH directly or indirectly inhibits primordial follicles from entering the pool of growing follicles. AMH is an important regulator that regulates the rate at which primordial follicles enter the growing pool, and knockout female mice exhibit premature depletion of primordial follicles and increase of ovarian size. (Visser et al., 2007, Durlinger et al., 1999). Therefore, it is used as a make for ovarian reservation. In humans, AMH significantly reduced the expression of follicle-stimulating hormone (FSH) -stimulated aromatase in granulosa cells and decreased the expression of FSH receptor mRNA, and regulating the ovarian follicular response

to gonadotropin (Sacchi et al., 2016). Additionally, using a mouse ovarian follicle culture system, it has been reported that AMH inhibits FSH-stimulated follicle growth by decreasing the sensitivity of follicles to FSH (Hayes et al., 2016). In cultured rat granulosa cells, exogenous AMH inhibits biosynthesis of aromatase, decreases the number of luteinizing hormone (LH) receptors, and prevents the proliferation of cultured granulosa-luteal cells (Durlinger et al., 1999).

The Hippo signaling pathway is essential for maintaining optimal organ size. Many studies have reported that the Hippo signaling pathway may also be involved in the regulation of mammalian ovarian functions. The studies in *Drosophila melanogaster* and mammals have shown that the pathway plays a critical role in controlling proliferation of granulosa cells, maturation of oocytes, follicular atresia in ovarian follicle growth and folliculogenesis (Lyu et al., 2016). Hippo pathway consists of several negative growth regulators acting in the kinase cascade (Kawamura et al., 2003). It is an evolutionarily conserved serine/threonine kinase signaling cascade originally identified in *Drosophila melanogaster* (Park et al., 2018). In terms of organ growth, Hippo pathway is gradually activated with increase in cell density as an organ or tissue grows (Hayashi et al., 2015). These include MST1/2 (mammalian Ste-20 like kinase), LATS1/2 (large tumor suppressor kinase), SAV1 (adaptor Salvador), and MOB1 (Mps one binder) which interfere with nuclear access of key effectors YAP (Yes-associated protein) and transcriptional coactivator WWTR1 (WW domain containing transcription regulator 1, also known as TAZ, PDZ-binding motif). (Grosbois, 2018).

When the Hippo signaling pathway is activated, MST1/2 complexes with SAV1 to phosphorylate the LATS1/2 kinases. Activated LATS1/2 form a complex with

their regulatory protein MOB1, and phosphorylate the transcriptional coactivator YAP/TAZ. Phosphorylated YAP/TAZ remains in the cytoplasm by binding with 14-3-3 or degrading in an ubiquitin-proteasome-dependent manner. In contrast, when Hippo pathway is inactivated, dephosphorylated YAP/TAZ translocate into the nucleus, where they bind to TEA domain family member (TEADs) to initiate target gene transcription and promote cell proliferation, survival and self-renewal. In addition to binding with TEADs, YAP/TAZ can also interact with other transcription factors, including SMADs, p73, Receptor tyrosine-protein kinase erbB-4 (ERBB4), Early growth response protein 1 (EGR-1), Runt-related transcription factor (RUNXs) and T-Box Transcription Factor 5 (TBX5) to regulate the expression of target genes (Kim et al., 2018). The activity of the Hippo pathway relies on cell-cell junctions, cell polarity, cellular architecture, cellular metabolism, and mechanical cues in the surrounding microenvironment (Barzegari et al., 2020).

Recently, the Hippo signaling pathway has been attracting attention as signaling pathways that are importantly involved in ovarian folliculogenesis. It has been suggested that the transient activation of YAP1 in the ovary could promote follicle growth, and LATS1 knockout cause of maintaining the primordial follicle pool (Lv, 2019). In vitro ovarian fragmentation decreased phosphorylated YAP levels, increased nuclear YAP, actin polymerization, and the expression of cellular communication network factor (CCN) 2 growth factor and baculoviral IAP repeat-containing protein (BIRC)1 (Kawamura et al., 2003). When ovarian tissue is fragmented in vitro, Hippo signaling is disrupted, and non-phosphorylated YAP enters the nucleus to interact with TEADs (Grosbois, 2018). Hippo signaling pathway forms a cross-network with various factors and

multiple signaling pathways such as Notch, TGFβ, cTGF, IGF, c-myc, and PI3K / AKt at various levels (Xiang, 2015).

Both Hippo and AMH are involved in folliculogenesis, interconnection in important roles of AMH and Hippo signaling is predicted and the information is very restricted. In this study, the activity of YAP/TAZ is investigated whether Hippo signaling interconnect to AMH-mediated folliculogenesis and confirmed the expression of *Ctgf, Areg, Id1* and *Ddit4*. In addition, the possible roles of Hippo and AMH was examined.

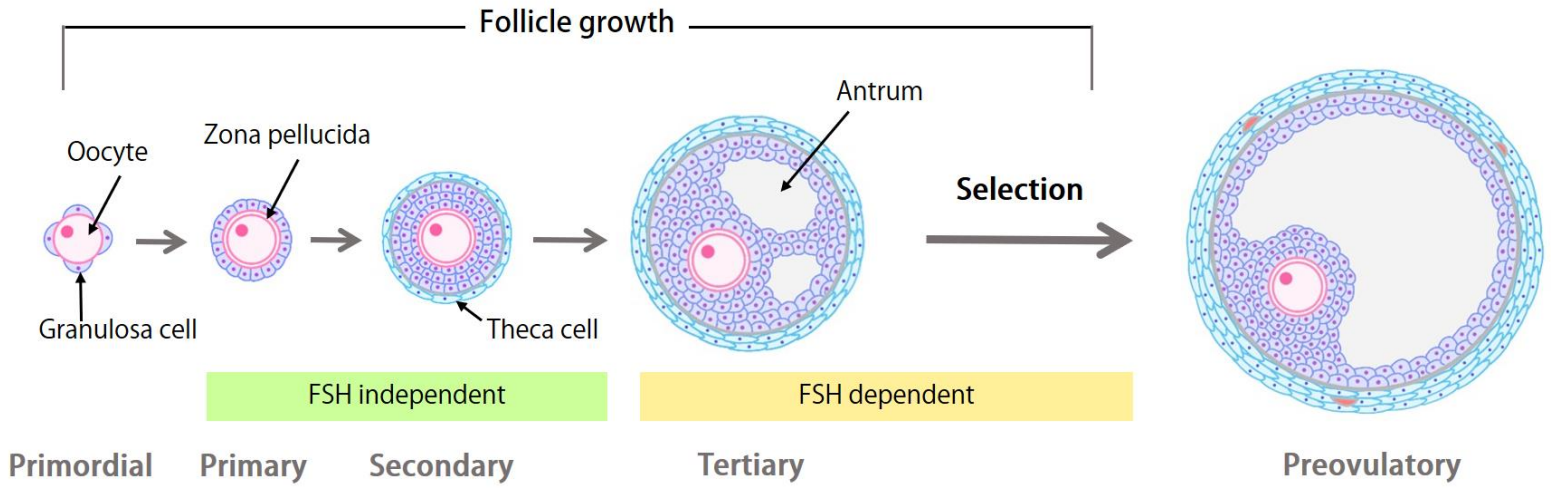

Figure 1. Diagram of ovarian folliculogenesis

The oocyte goes through a process called folliculogenesis until ovulation. Follicular stages were defined as primordial follicles (follicles with single layer of flattened granulosa cells surrounding an oocyte), primary follicles (follicles with single layer of cuboidal granulosa cells), secondary follicles (follicles with two or more layers of cuboidal granulosa cells), tertiary follicles (follicles where a cavity in the granulosa cells appear or antrum formation begins), preovulatory follicles (follicles with large antrum).

MATERIALS AND METHODS

Experimental animals

All experimental animals were conducted according to the Guide for the Care and Use of Laboratory Animals published by the National Institute of Health (NIH). All experiments were approved by the Institutional Animal Cars Use Committee (IACUC) in Sungshin Women's University (SSWIACUC-2021-002). 6-8-weeks-old C57BL/6, heterozygous and homozygous B6;129S7-AMH$^{tm1Bhr/J}$ female mice were maintained under the light-on at 6:00 am and light-off at 7:00 pm, and clean room system. Animals were fed a standard rodent diet and water ad libitum from weaning at 28 days after birth.

In vivo ovarian resection

The mice were anesthetized with pentobarbital sodium (97.5 mg/kg). After dressing with 70% Et-OH, small incision in the skin of the right back was made using scissors, and the right ovary was pulled out using forceps. Under the microscope, the ovary was resected with micro-scissors one-third (1/3 group) or two-third (2/3 group) (Fig. 2). The ovary was returned inside the cavity, and the skin was sutured. Partial ovarian resection was performed only on the right ovary with the contralateral left ovary unoperated as a control. Mice were sacrificed at 0 h, 1 h, 12 h, 24 h, 96 h and 144 h, respectively, and paired ovaries were collected for analysis.

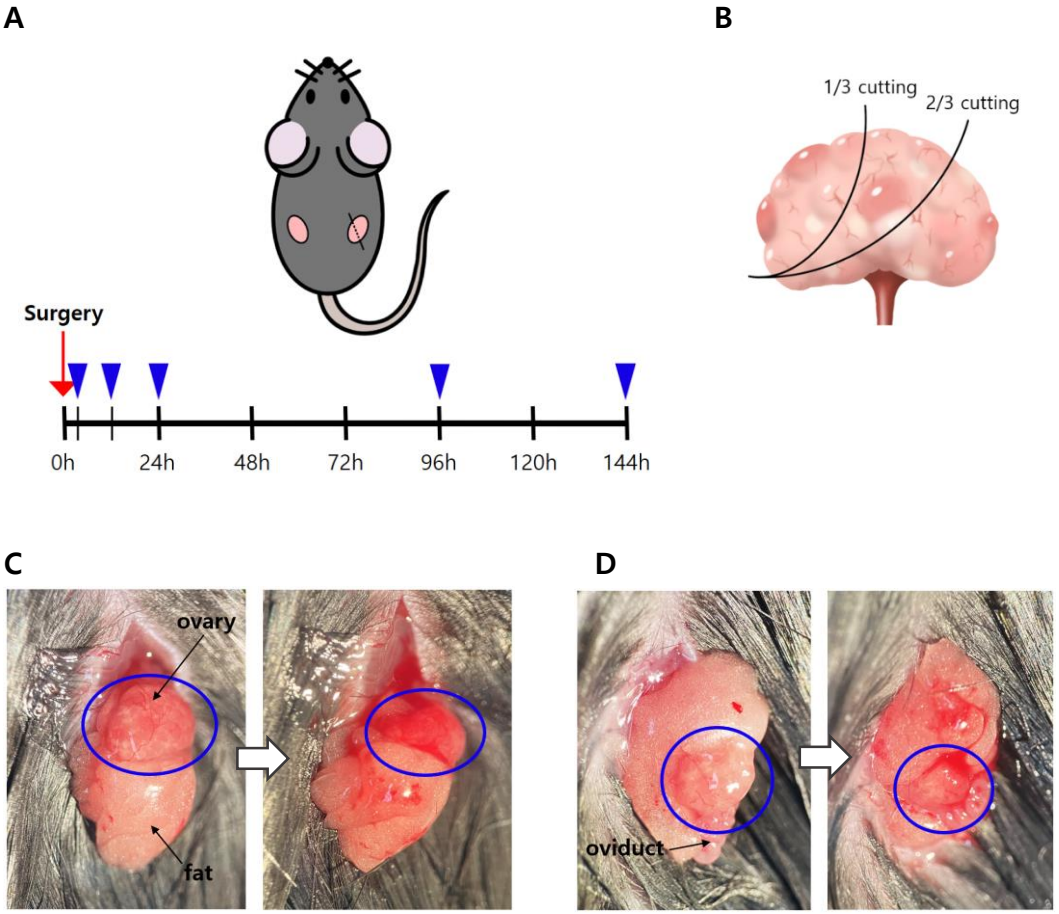

Figure 2. Overview of the partial resection of the ovary

(A) Timeline for sampling ovaries after surgery. One-third or two-third of one ovary of a pair was resected and the contralateral ovary was remained undamaged as control. Ovaries were collected at 0 h, 1 h, 12 h, 24 h, 96 h and 144 h after surgery. (B) The cutting scheme of ovary. (C, D) View of the ovary before and after one-third (C) and two-third (D) excision.

Total RNA extraction

Ovaries were homogenized in TRIzo® reagent (Invitrogen, Cat #: 15596-026, Massachusetts, USA) (1 ml / 0.1 g) for 30 seconds and stored for 10 min at room temperature (RT). Next chloroform of 0.2 ml / 1 ml TRIzol reagent added in homogenized tube and vigorously shake at 15 seconds and stored for 15 min at RT. And centrifuged 12,000 *g* for 15 min at 4℃. Supernatant was transferred to new tube, and added 0.5 ml of isopropanol in 1 ml TRIzol, mixed gently and kept for 10 min at RT. Then centrifuged 12,000 *g* for 8 min at 4℃. The supernatant was removed and RNA pellet were floated in 1ml 75% Et-OH by inverting, and centrifuged 7,500 *g* for 5 min at 4℃. The supernatant was removed, dried to remove ethanol for 4 min at RT, and added 50 μl 0.1% DEPC treated water.

cDNA synthesis

Briefly, reaction reagents are 34 μl total RNA, 10 μl MMLV 5X buffer, 1 μl oligo dT primer (0.5 μg/μl), 1 μl random primer (0.1 μg/μl), 2 μl dNTP mix (100 mM). Reaction mixture was incubated at 65℃ for 5 min, placed the tube at RT for 5 min, and then added 4.5 μl DTT (100 mM), 2 μl M-MLV Reverse Transcriptase (Promega, Cat#: M170B, Wisconsin, USA), 1 μl RNase block ribonuclease inhibitor (40 U/ml). The mixture was incubated at 42℃ for 1 hr and 70℃ for 15 min to terminate cDNA synthesis. And kept -20℃ before it used.

Real-time PCR analysis

For quantification of expression levels, transcripts of target genes were amplified using reverse transcript(RT)-PCR and the specific primers (Table 2).

Quantification real time RT-PCR was performed using SYBR Premix Ex Taq™ (TaKaRa, Cat#: RR420, Shiga, Japan) and AriaMx Real-time PCR System (Agilent, Cat#: G8830A California, USA). Information of the thermal cycle are in Table 1. Each reaction was run in triplicate and consisted of 1 μl cDNA. Dissociation curves were run on all reactions to ensure amplification of a single product with the appropriate melting temperature. The fold change in gene expression was calculated using the ΔΔCt method with the housekeeping gene, ribosomal protein, *36B4*, as the internal control.

Protein extraction and Western blotting analysis

Ovaries were homogenized in cold homogenization buffer (50 mM Tris-Cl, 150 mM NaCl, 10 mM β-mercaptoethanol, 2 mM CaCl2, 0.1 mM PMSF, 1μM Leupeptin, 1 μM Pepstatin, 0.5 mM EDTA, 15% Glycerol, and 0.1% NP-40). The homogenates were centrifuged to remove insoluble materials. The protein concentration was determined by BCA assay using protein dye reagent (Thermo Fisher scientific, Cat#: 23225, Massachusetts, USA). 20 μg /ml of protein were boiled in SDS/β-mercaptoethanol sample buffer, and loaded onto each lane of 10% SDS-PAGE. The proteins were separated by electrophoresis and then electrotransferred onto polyvinylidene difluoride (PVDF) membranes (Bio-Rad, Cat#: 1620177, California, USA) in transfer buffer (25 mM Tris base, 192 mM Glycine, 0.1% SDS, and 20% Methanol, pH 8.3). The membranes were blocked in 10% skimmed dry milk in TBST buffer (10 mM Tris-HCl, 150 mM NaCl and 0.05% Tween-20) for 1 hr at RT, and washed three times with TBST. The membranes were incubated during overnight with rabbit monoclonal YAP/TAZ antibody (dilution 1:1000); rabbit polyclonal p-YAP antibody (dilution 1:1000);

rabbit monoclonal GAPDH antibody (dilution 1:2000) at 4℃. After incubation, membranes were washed three times and incubated for 1 hr with horseradish peroxidase conjugated goat anti-rabbit IgG (dilution 1:5000); goat anti-mouse IgG-HRP (dilution 1:5000) for 1 hr. The bands were detected using ECL solution (Bio-Rad, Cat#: 1705060, California, USA) by ChemiDoc MP Imaging System (Bio-Rad, Cat#: 17001402, California, USA). The intensity of each band was normalized with total protein using ImageJ software. Information of the antibodies is presented in Table 3.

Ovarian follicle counting

Ovaries were fixed in 4% paraformaldehyde with picric acid at 4℃. The overnight-fixed ovaries were dehydrated in alcohol series, and embedded in paraffin using Leica EG1150H. The pasaffin block was serial-sectioned at 4 μm using Leica RM2245 microtome and every 10th sections were stained with hematoxylin and eosin Y. Tissue were microphotographed using Leica Labovert microscope and Nikon digital sight DS-Fi1 microscope digital camera. Follicles were identified as normal if they contained an intact oocyte, organized granulosa and thecal cell layers, and no pyknotic bodies. Adopting the following calassification, follicular stages were defined as (1) primordial follicles: follicles with one layer of flattened granulosa cells surrounding an oocyte, (2) Primary follicles: follicles with one layer of cuboidal granulosa cells, (3) Secondary follicles: follicles with two or more layers of cuboidal granulosa cells, (4) Tertiary follicles: follicles where a cavity in the granulosa cells appear and/or antrum formation begins, (5) Preovulatory follicles: follicles with large antrum (Fig. 1).

Immunohistochemistry

4 μm sections were mounted on glass slides and subjected to antigen retrieval in boiling 10mM sodium citriate buffer (pH 6.0) for 15 min. Endogenous peroxidase activity was blocked in 0.3% hydrogen peroxide in H_2O for 10 min. YAP immunoreactivity was detected according to the VECTASTAIN® Elite ABC-HRP kit, Peroxidase (Rabbit IgG) (Vector Laboratories, Cat#: PK-6101, California, USA) method. Briefly, tissues were incubated with 1% normal goat blocking serum in 0.1% BSA in PBS for 1 hr. And then samples were incubate with rabbit monoclonal YAP/TAZ antibody (dilution 1:200) in 0.1% BSA in PBS during overnight at 4℃. Next day, washing in PBST; Tissues were incubated with biotinylated anti-rabbit IgG (dilution 1:250) in 0.1% BSA in PBS for 1 hr; Tissues were washed with PBST and PBS; Incubated with avidin-biotin complex regeant containing horseradish peroxidase for 30 min. Slides were washed with PBST and PBS. And color development was achieved using DAB (Vector Laboratories, Cat#: SK-4100, California, USA) substrate. And then the tissues were conter stained with hematoxylin.

Statistics

All experiments were conducted at least in triplicate. The Student's t-test, one-way ANOVA and Tukey's multiple-comparison test was performed to evaluate the statistical significance between control and experiment group. Results were presented as mean ± standard errors of the means (SEM). Values of $P < 0.05$ were considered to be significantly different. All analyses were done using IBM SPSS statistic 25.

Table 1. Real-time RT-PCR Thermal cycler schedule

Step		Temperature(℃)	Time	cycles
Hold		94	30 min	1
3 steps PCR	Denaturation	95	1 min	45
	Annealing	59	30 sec	
	Extension	72	1 min	
Dissociation	Denaturation	95	15 sec	1
	Annealing	60	30 sec	
	Extension	95	15 sec	
Hold		4	Indefinitely	1

Table 2. Primer sequences for quantitative real-time PCR

Gene	Symbol	NCBI gene reference		Primer sequence (5'-3')	Amplified length (bp)
Yes1 associated transcriptional regulator	***Yap1***	NM_001171147.1	S	GACTTGGAGGCGCTCTTCAAT	230
			AS	GAACATGCTGTGGAGTCAGAGCT	
WW domain containing transcription regulator 1	***Wwtr1 (TAZ)***	NM_001168281.1	S	TCGCAGGAACTTGCGTTACA	231
			AS	TTCCTGGACCAAGCTGCCTA	
Connective tissue growth factor	***Ctgf***	NM_010217.2	S	TTGGCCCAGACCCAACTATG	232
			AS	TTGACAGGCTTGGCGATTTT	
Amphiregulin	***Areg***	NM_009704.4	S	TGTTGCTGCAGAGACCGAGA	225
			AS	GGCATTTCGCTTATGGTGGA	
DNA damage inducible transcript 4	***Ddit4***	NM_029083.2	S	GCCTAGCCTCTGGGATCGTT	220
			AS	GGGACACCCCATCCAGGTAT	
Inhibitor of DNA binding 1	***Id1***	NM_001355113.1	S	GCCCTAGCTGTTCGCTGAAG	243
			AS	CCTTGCTCACTTTGCGGTTC	
TEA Domain Transcription Factor 1	***Tead1***	NM_001166584.2	S	ATCCATTGGCACAACCAAGC	211
			AS	GCCCTTTCCAAACAGCTCCT	
SMAD family member 1	***Smad1***	NM_008539.4	S	GTCCCACCGGAAGGGACTAC	230
			AS	ACTGAGCCAGAAGGCTGTGC	
SMAD family member 2	***Smad2***	NM_010754.5	AS	TAGGTGGGGAAGTGTTTGCTGA	221
			S	GTGCACATTCGGGTTAGCTGAT	
60S acidic ribosomal protein P0	***Rplp0 (36B4)***	NM_007475	S	CGACCTGGAAGTCCAACTACTTCCT	303
			AS	GCACCTTATTGGCCAACAGCAT	

Table 3. Antibody information

Antibody	Description	Cat #	Company
YAP/TAZ	Rabbit monoclonal	#8418	Cell signaling
p-YAP	Rabbit polyclonal	orb99152	Biorbyt
GAPDH	Mouse monoclonal	sc-32233	Santacruz

RESULTS

Age dependent fertility in anti-Müllerian hormone knockout mice

Wild type female mice and *Amh* null female mice were bred with wild type males for two weeks, and pregnant mice were recorded. Delivery rates in wild type female mice: ≥ 6wk was 66.67%, ≥ 3m was 73.33%, ≥5m was 66.67% and ≥ 7m was 51.43% (Fig. 3). Delivery rate was decreased by aging. In *Amh* KO female mice the delivery rates: ≥ 6wk was 53.33%, ≥ 3m was 76.92%, ≥ 5m was 68.75% and ≥ 7m was 41.94% (Fig. 3). Delivery rate was dropped by aging (≥ 7m) likes in wild type mice but more sharply.

.

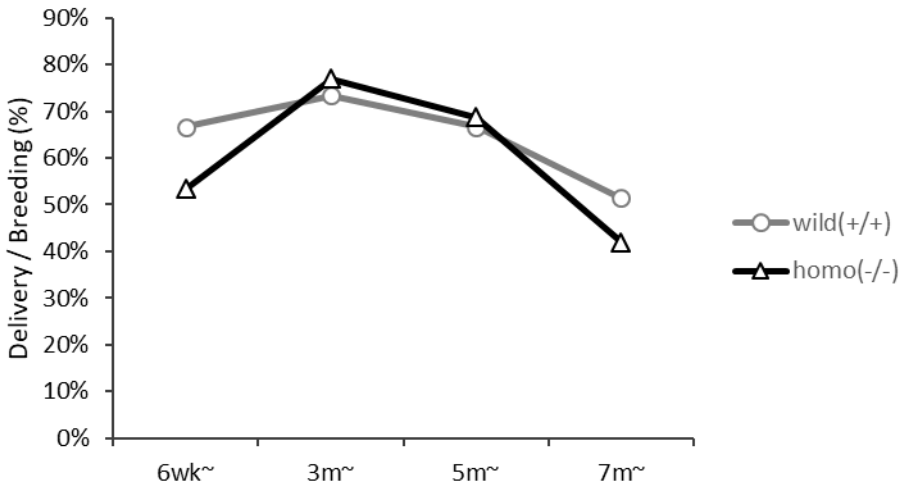

Figure 3. Female age-and genotype-dependent delivery rate

Statistical significance between genotypes was assessed by chi-square test at $P < 0.05$.

Changes in the weight of the mouse ovary after resection

The weight of the ovaries gradually increased to 5 months, and then began to decrease after 5 months. At 6 weeks the weight of the mouse ovary compared to the body weight was 0.21 ±0.06, 0.24 ±0.02 at 3 months, 0.26 ±0.05 at 5 months, 0.24 ±0.02 at 7 months, and 0.13 ±0.003 at 12 months (Fig. 4). The 1/3 or 2/3 groups were sampled at 0, 1, 12, 24, 96, and 144 h to measure the weight. The intact ovaries on the opposite side were sampled at the same time and the weight changes were compared. In the 1/3 group, the ovarian weight increased over time for both the cut and intact ovaries. The weight increased significantly after 144 h after resection of a part of the ovary (Fig. 5A). The 2/3 group and the *Amh* KO 1/3 group also showed an increase in ovarian weight at 144 h after surgery, but there was no significant difference (Fig. 5B, C). The *Amh* KO 1/3 group showed relatively less weight gain than the wild type group. The slope was calculated by representing the weight change as a trend line. The wild type 1/3 group had 0.0093 intact ovaries and 0.0112 cut ovaries, 2/3 wild type 0.0064, 0.0031, and the *Amh* KO 1/3 group 0.005, 0.0058.

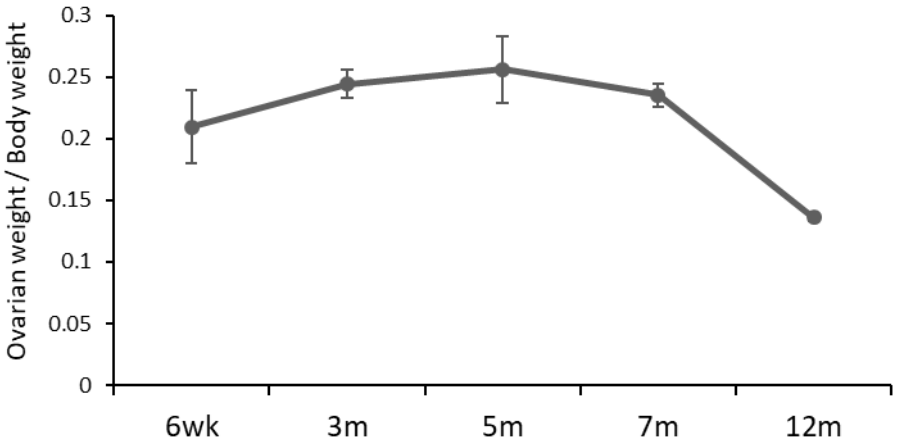

Figure 4. Reproductive age dependant mouse ovarian weight

The weight of each ovary of mouse was measured and divided by the body weight. 6wk is 6 weeks old, 3m is 3 months old, 5m is 5 months old, 7m is 7 months old and 12m is 12 month old. Data are represented as the mean ±SEM.

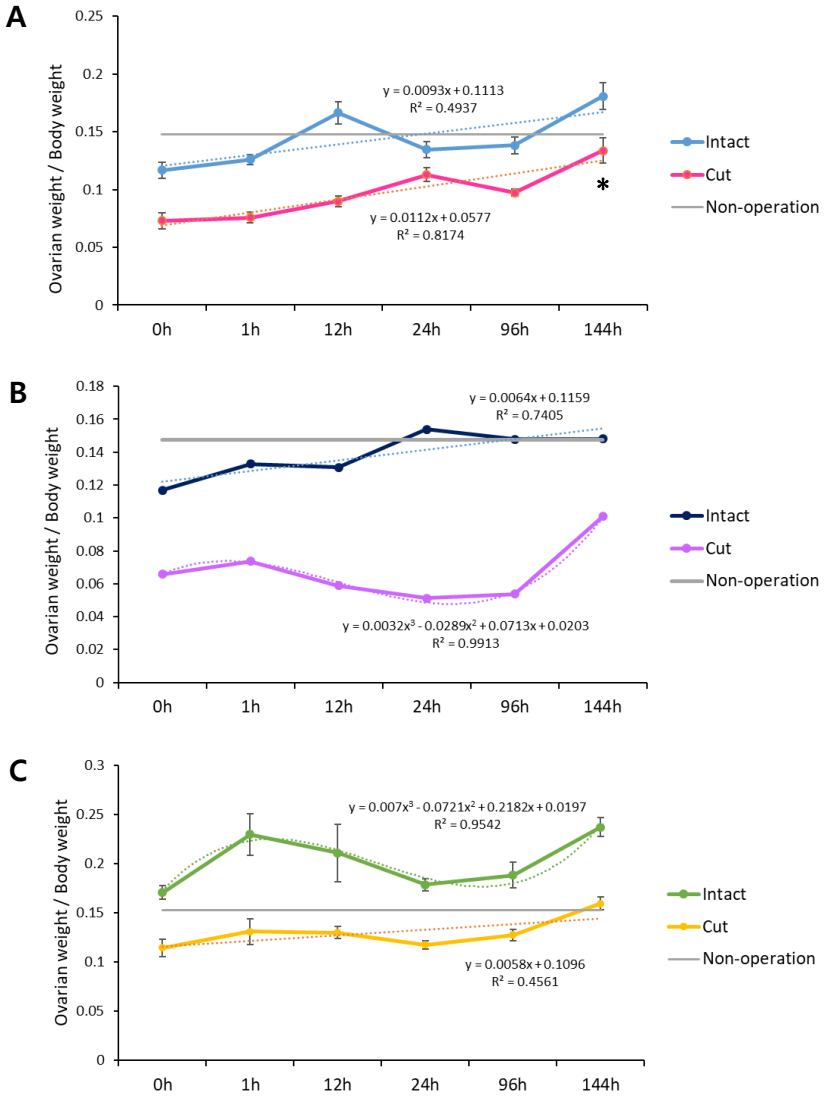

Figure 5. Comparison of ovarian size after surgery

Weight change of the mouse ovary after one-third (A) and two-third (B) excised surgery. (C) Weight change of the *Amh* knockout mouse ovary after one-third excised surgery. Gray line indicates the mean ovarian weight of non-operative mice. The dotted line represents the trend line of the graph and its equation. *: $p < 0.05$ (0 h to each groups). Data are represented as the mean ±SEM.

Yap, Taz and *Tead1* mRNA expression profile of wild type 1/3 and 2/3 ovaries and anti-Müllerian hormone knockout ovaries

After cutting the mouse ovaries, quantitative real-time PCR analysis was performed to examine transcriptional changes in the *Yap*, *Taz* gene in wild-type (WT) and *Amh* knockout (KO) mice. In addition, mRNA expression was compared between the wild type ovary from which 1/3 was excised and the ovary from which 2/3 was excised. When YAP/TAZ is activated, it moves to the nucleus and interacts with the TEADs transcription factor to form a complex. TEADs are the key effector of the Hippo signaling pathway and the best-characterized binding partner of YAP/TAZ. Therefore, the transcriptional changes in the TEAD1 gene were also investigated. *Yap* mRNA was not significantly changed in the WT 1/3 cut ovary (Fig. 6A). After resection from the WT 2/3 cut ovary, *Yap* mRNA expression was significantly reduced at 0 h, 12 h, 96 h and 144 h. In *Amh* KO 1/3 cut ovaries, *Yap* mRNA expression decreased at 0 h and 12 h after excision.

Taz mRNA expression was significantly increased at 0 h in the WT 1/3 cut (Fig. 6B). In WT 2/3, it increased significantly to 0 h, 1 h, 12 h, and 24 h, and then appeared at the same level as the complete ovary. In *Amh* KO 1/3, *Taz* mRNA expression decreased to 0 h and 12 h after excision but increased significantly to 96 h.

The mRNA expression of *Tead1* was significantly reduced only at 0 h of *Amh* KO 1/3 (Fig. 16C). These data indicate that 1/3 resection of the ovaries of wild type and *Amh* KO mice cannot affect the mRNA expression of *Yap, Taz,* and *Tead1.* After excision of 2/3, the expression of *Yap* mRNA decreased after excision, and *Taz* mRNA increased first and returned to the baseline.

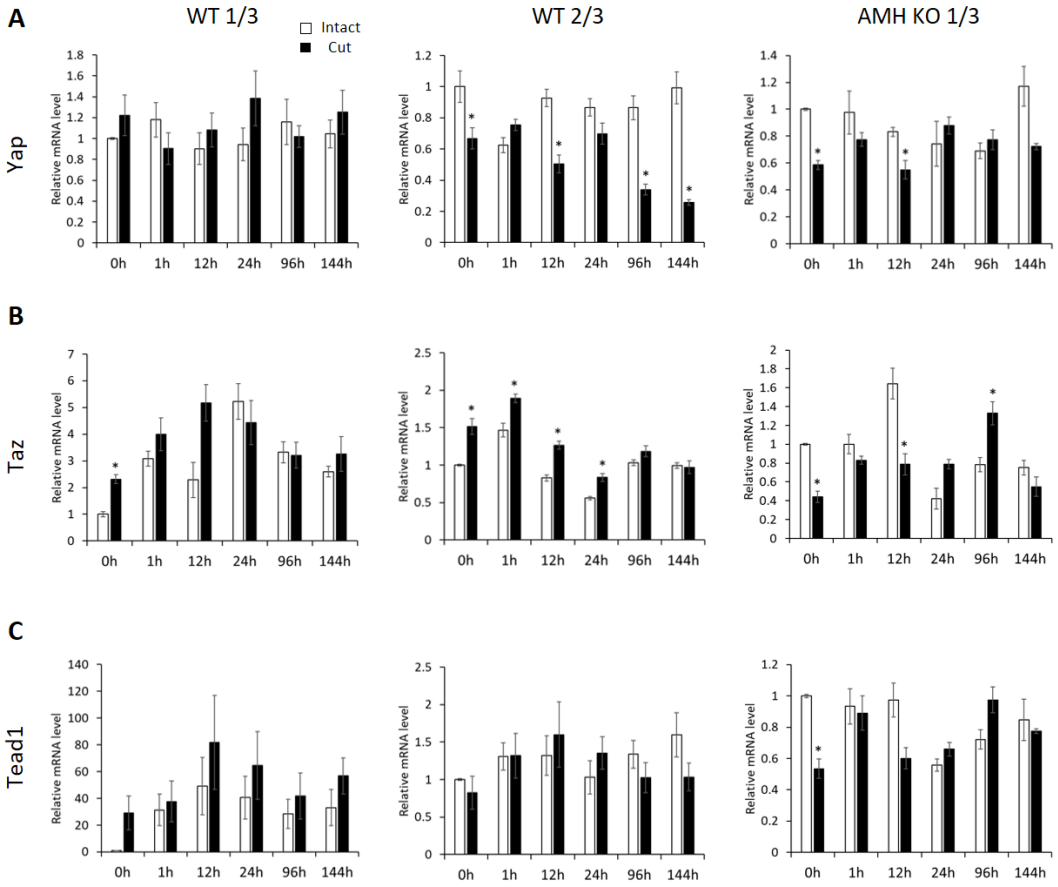

Figure 6. Transcriptional analysis of *Yap*, *Taz* and *Tead1* on mouse ovaries

Relative *Yap* mRNA (A), *Taz* mRNA (B) and *Tead1* mRNA (C) expression level changes in wild type 1/3 and 2/3 cut ovaries and *Amh* KO 1/3 cut ovaries. Gene expression was calculated using the ΔΔCt method with the *36B4*, as the internal control. *: $p < 0.05$ (0 h to each groups). Data are represented as the mean ±SEM.

Protein expression profiles of wild type 1/3 and 2/3 ovaries and anti-Müllerian hormone knockout ovaries

Western blotting analysis was performed to determine the protein expression levels of YAP/TAZ and phosphorylated YAP (Ser 127) in mouse ovaries. When compared with intact ovaries, YAP protein expression was significantly increased 96 h and 144 h after resection, and was also significantly increased compared to ovary after 0 h resection. The WT 2/3 group showed an increase in YAP expression immediately after resection compared to the intact ovary, but no significant change thereafter (Fig. 7B). In the *Amh* KO 1/3 group, YAP protein expression was increased 24 h and 144 h after resection (Fig. 7C).

Expression of TAZ protein was significantly increased in the WT 1/3 group at 144 h (Fig. 8A). After excision, there was a significant increase at 96 h and 144 h compared to 0 h. In the WT 2/3 group, TAZ increased immediately after excision and showed no significant change thereafter (Fig. 8B). The *Amh* KO 1/3 group also had a significant increase in TAZ protein after 144 h (Fig. 8C). However, in the WT 1/3 group, the expression of YAP/TAZ after resection 144 h was 3.59 and 3.04, respectively, and *Amh* KO 1/3 was 1.22 and 1.23, and protein expression was relatively higher in WT 1/3.

The level of p-YAP in the WT 1/3 group was significantly reduced after 144 h of resection (Fig. 9A). In the WT 2/3 group, it decreased significantly immediately after resection and then increased (Fig. 9B). In the *Amh* KO 1/3 group, p-YAP levels were significantly reduced after 144 h of excision (Fig. 9C).

These data suggest that the expression level of YAP/TAZ does not increase with the volume of excised ovaries, and that it is relatively low in *Amh* KO mice compared to wild type mice. Furthermore, it is suggested that Hippo signaling, which is altered by excision of the ovaries, occurs at the protein level rather than the mRNA level.

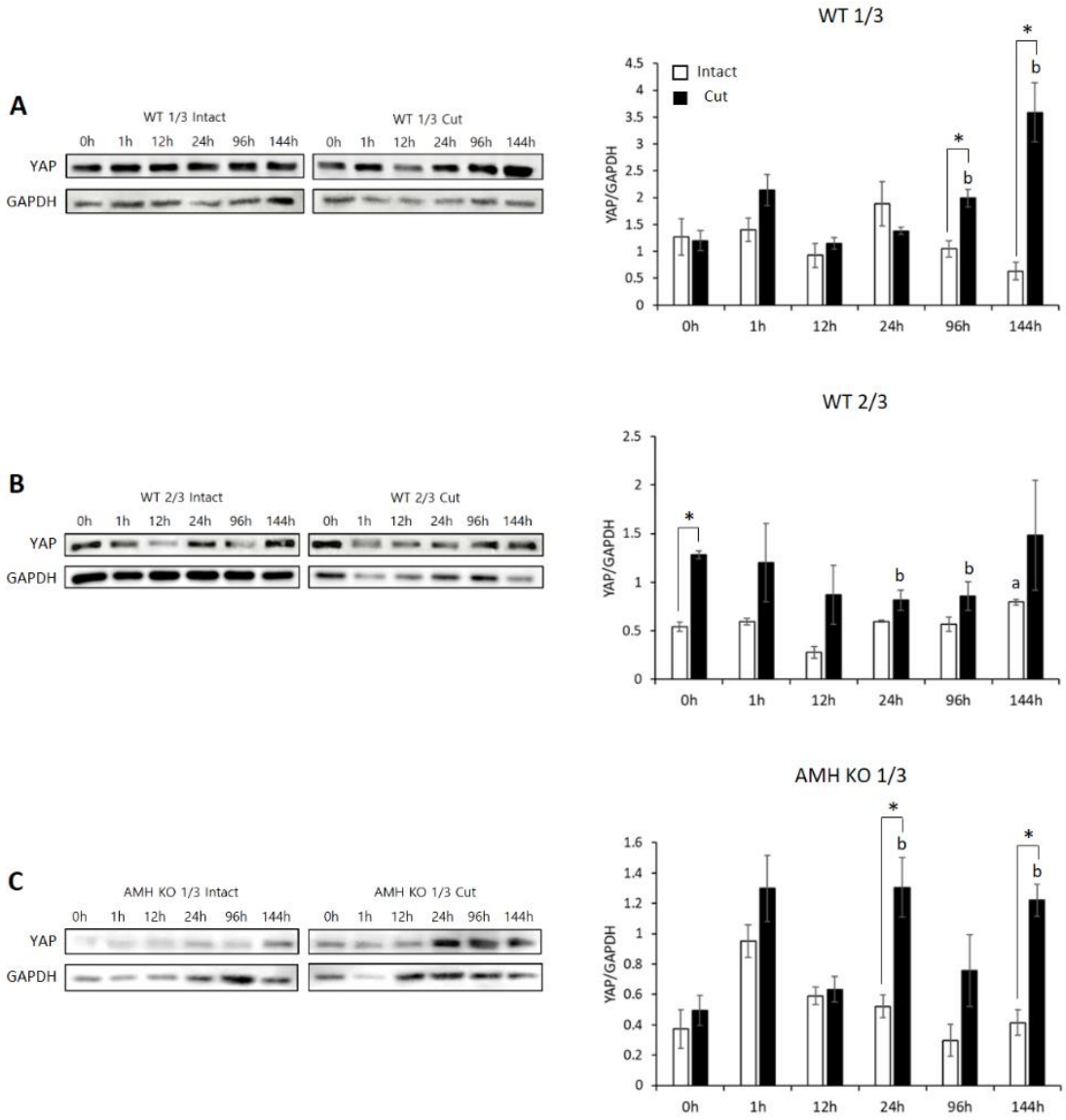

Figure 7. YAP protein expression profiles on mouse ovaries

Western blotting analysis of ovaries of 1/3 cut (A), 2/3 cut (B) wild type and 1/3 cut *Amh* KO (C) for YAP. The target protein levels were normalized to GAPDH. *: $p < 0.05$ (Intact group vs Cut group). a: A significant difference between intact ovaries. b: A significant difference between cut ovaries. Data are represented as the mean ±SEM.

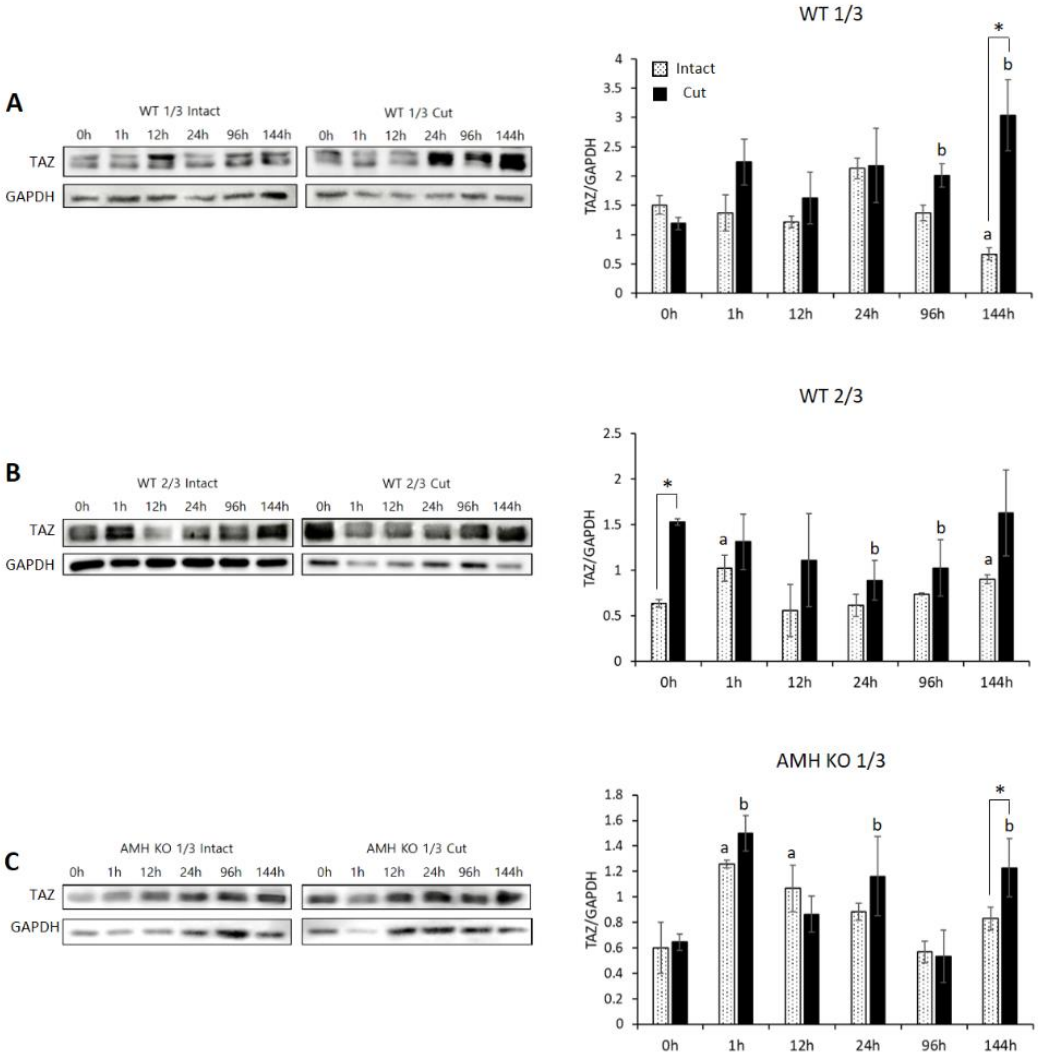

Figure 8. TAZ protein expression profiles on mouse ovaries

Western blot analysis of ovaries of 1/3 cut (A), 2/3 cut (B) wild type and 1/3 cut *Amh* KO (C) for TAZ. The target protein levels were normalized to GAPDH. *: $p < 0.05$ (Intact group vs Cut group). a: A significant difference between intact ovaries. b: A significant difference between cut ovaries. Data are represented as the mean ±SEM.

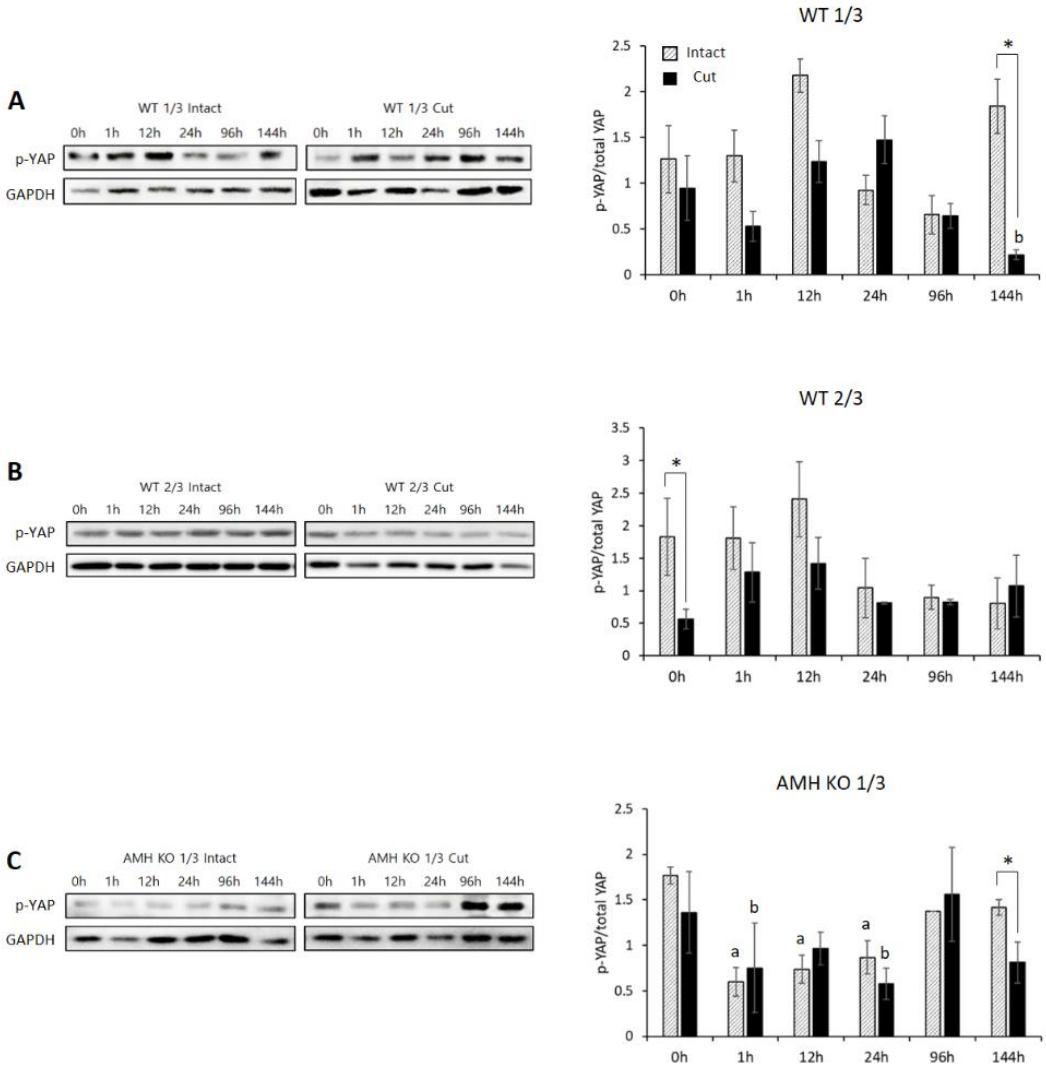

Figure 9. Phosphorylated YAP (Ser 127) expression profiles on mouse ovaries

Western blot analysis of ovaries of 1/3 cut (A), 2/3 cut (B) wild type and 1/3 cut *Amh* KO (C) for p-YAP. The target protein levels were normalized to GAPDH. *: $p < 0.05$ (Intact group vs Cut group). a: A significant difference between intact ovaries. b: A significant difference between cut ovaries. Data are represented as the mean ±SEM.

YAP/TAZ target gene mRNA expression profiles of wild type 1/3 and 2/3 ovaries and anti-Müllerian hormone knockout ovaries

To further investigate the expression of YAP/TAZ, the target gene mRNA expression level of YAP/TAZ was analyzed by real time PCR analysis. Connective tissue growth factor (CTGF) is the most well-known target gene for YAP/TAZ/TEADs complex.

Ctgf mRNA level increased 144 h after resection in the WT 1/3 group, but not significant. In the WT 2/3 group, there was decrease at 0 h, 12 h, and 144 h. The *Amh* KO 1/3 group also increased to 144 h, but not significant. Amphiregulin *(Areg)* mRNA expression increased to 1 h, 12 h and 24 h in the WT 1/3 group. In the WT 2/3 group, it increased to 1 h and decreased to 144 h. The *Amh* KO 1/3 group also increased to 1 h, but decreased at 12 h, 96 h and 144 h. The mRNA level of inhibitor of DNA binding 1 *(Id1)* tended to decrease compared to the intact ovary in the WT1/3 group, and increased after 144 h in the WT2/3 group. No significant changes were seen in the *Amh* KO 1/3 group. DNA damage inducible transcript 4 *(Ddit4)* mRNA levels were reduced at excision 96 h and 144 h in the WT 1/3 group. The WT 2/3 group constantly decreased up to 144 h after resection, with no significant difference in the *Amh* KO 1/3 group. This change in transcriptional levels of the YAP/TAZ target gene indicates a relatively increased activity of YAP/TAZ in the WT 1/3 group.

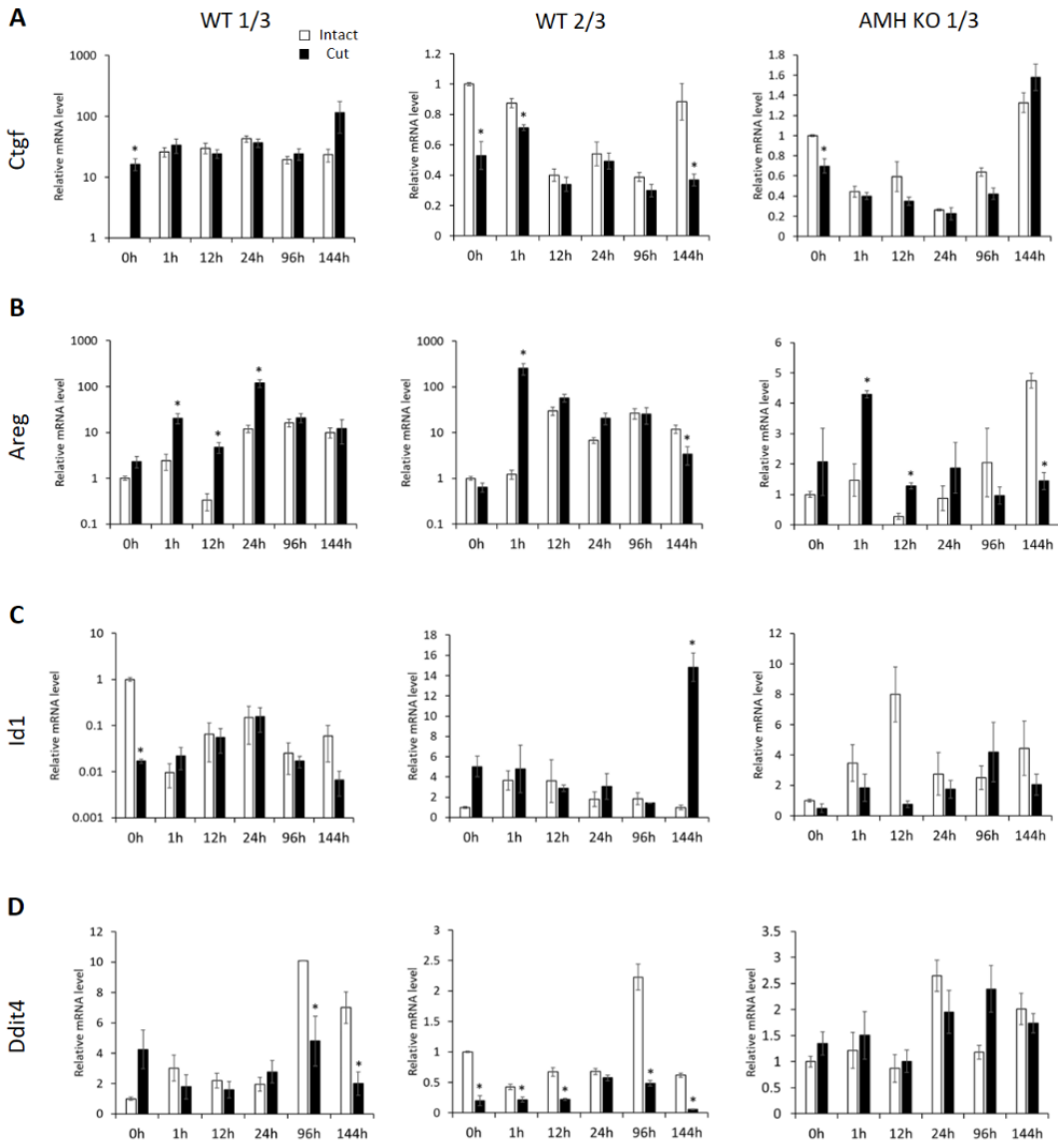

Figure 10. Transcriptional analysis YAP/TAZ target genes on mouse ovaries

Relative *Ctgf* mRNA (A), *Areg* mRNA (B), *Id1* mRNA (C) and *Ddit4* mRNA (D) expression level changes in wild type 1/3 and 2/3 cut ovaries and *Amh* KO 1/3 cut ovaries. Gene expression was calculated using the ΔΔCt method with the *36B4*, as the internal control. *: $p < 0.05$ (0 h to each groups). Data are represented as the mean ±SEM.

Smads mRNA expression profiles of wild type 1/3 and 2/3 ovaries and anti-Müllerian hormone knockout ovaries

SMADs are transduce extracellular signals from TGF-β to the nucleus and activate transcription of downstream target genes. It is known that SMAD 1/5/8 combines with AMHRII to form a TGF-β signaling pathway (Beck et al., 2016), and SMAD 2/3 interacts with YAP/TAZ (Nakamura et al., 2021). Therefore, mRNA expression was investigated to determine whether SMADs were involved in the interconnection of Hippo signaling pathway and AMH. *Smad1* mRNA levels did not show any significant change at 0 h after resection in the WT 1/3 group (Fig. 11A). In the WT 2/3 group, there was a continuous significant decrease after resection, and in the *Amh* KO 1/3 group, there was no change except for 24 h. *Smad2* mRNA level increased continuously in WT 1/3, with no significant change after 0 h in WT 2/3 group (Fig. 11B). In the *Amh* KO 1/3 group, it decreased significantly up to 12 h and then increased. This result indicates that *Smad2* mRNA expression increases with increasing activity of YAP, suggesting the possibility of SMADs involvement in Hippo signaling pathway.

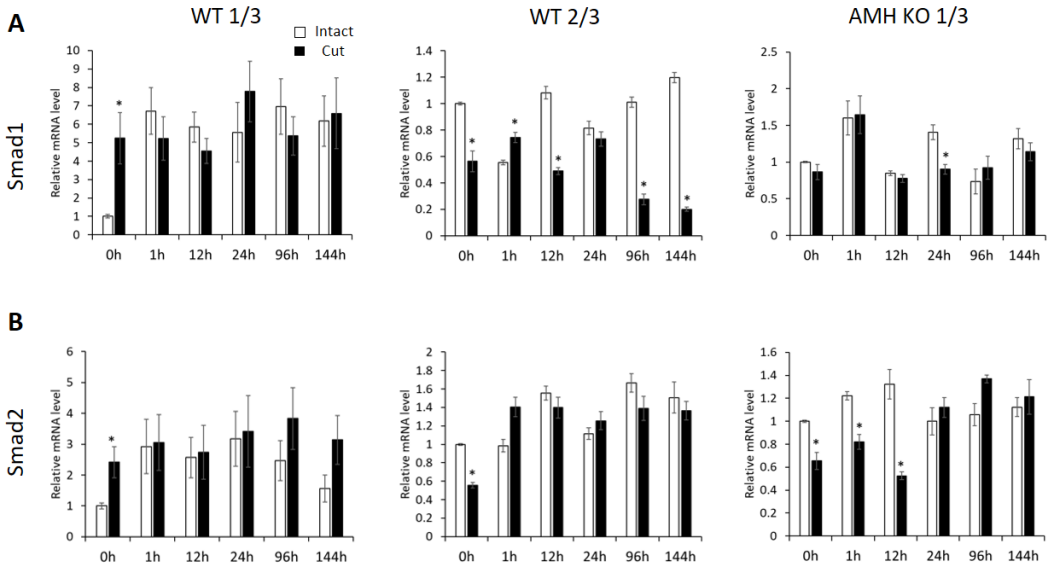

Figure 11. Transcriptional analysis *Smads* on mouse ovaries

Relative *Smad1* mRNA (A) and *Smad2* mRNA (B) expression level changes in wild type 1/3 and 2/3 cut ovaries and *Amh* KO 1/3 cut ovaries. Gene expression was calculated using the ΔΔCt method with the *36B4*, as the internal control. *: $p < 0.05$ (0 h to each groups). Data are represented as the mean ±SEM.

YAP/TAZ localization in mouse ovaries

After resection of the mouse ovaries, changes in YAP/TAZ localization were investigated by immunohistochemistry. In wild type ovary, YAP/TAZ was expressed throughout the ovary, but showed strong signals mainly in the granulosa cell nucleus of the follicle (Fig. 12A, B). Among follicles, the expression was relatively high in the secondary and tertiary follicles. It was also expressed relatively weakly in corpus luteum, and was mainly located in the cytoplasm of luteal cells. Expression of YAP/TAZ was also observed in the area where the ovaries were resected. After 24 h, follicle growth was promoted with strong expression of YAP/TAZ at the cut site. In the *Amh* KO ovary, it was mainly located in the nucleus of the granulosa cells, and YAP/TAZ was expressed in the excised part (Fig. 13A, B). There was no difference in YAP/TAZ localization between wild-type mice and *Amh* KO mice.

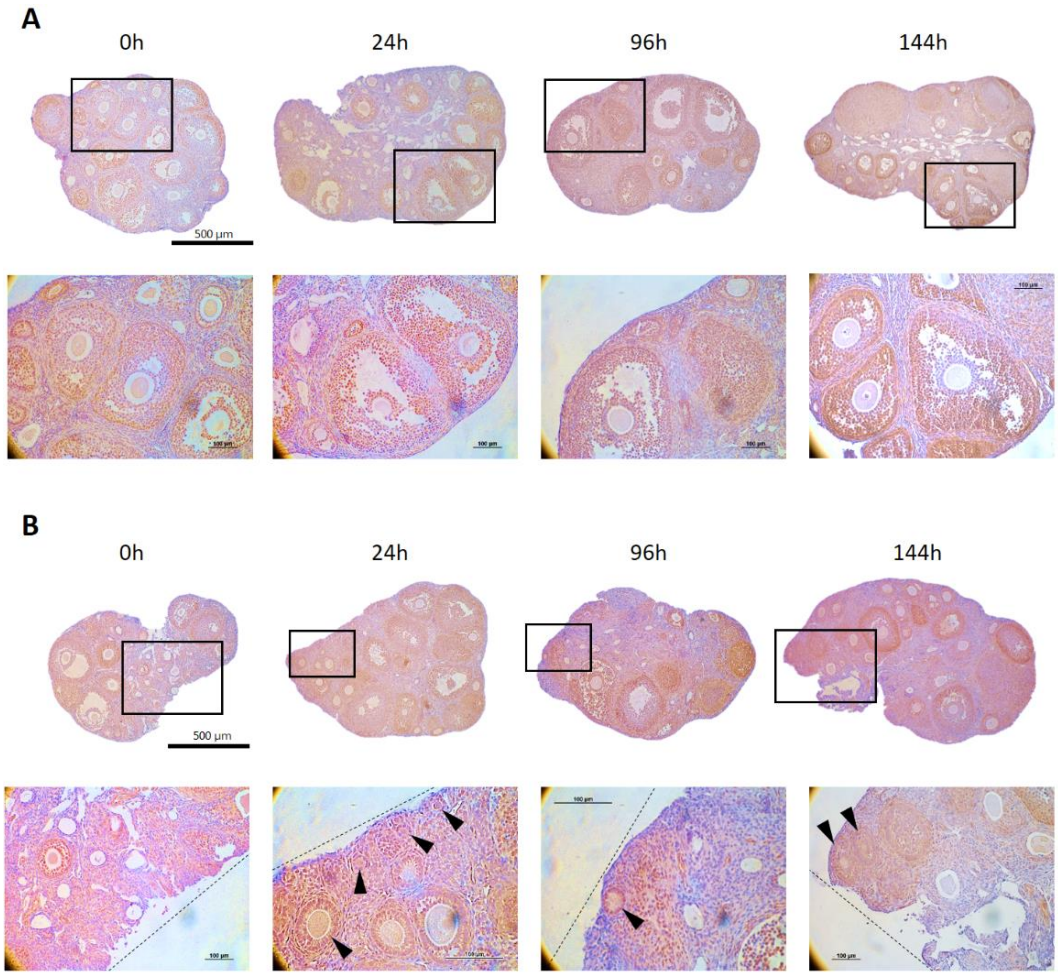

Figure 12. Immunohistochemistry of YAP/TAZ in wild type mouse ovaries

The expression of YAP/TAZ in wild mouse ovaries was histologically compared. (A) Intact ovaries. (B) Cut ovaries. Enlarged details as indicated by the black squares. Arrow heads indicate primary and secondary follicles. The scale bar in the enlarged figure represents 100 μm.

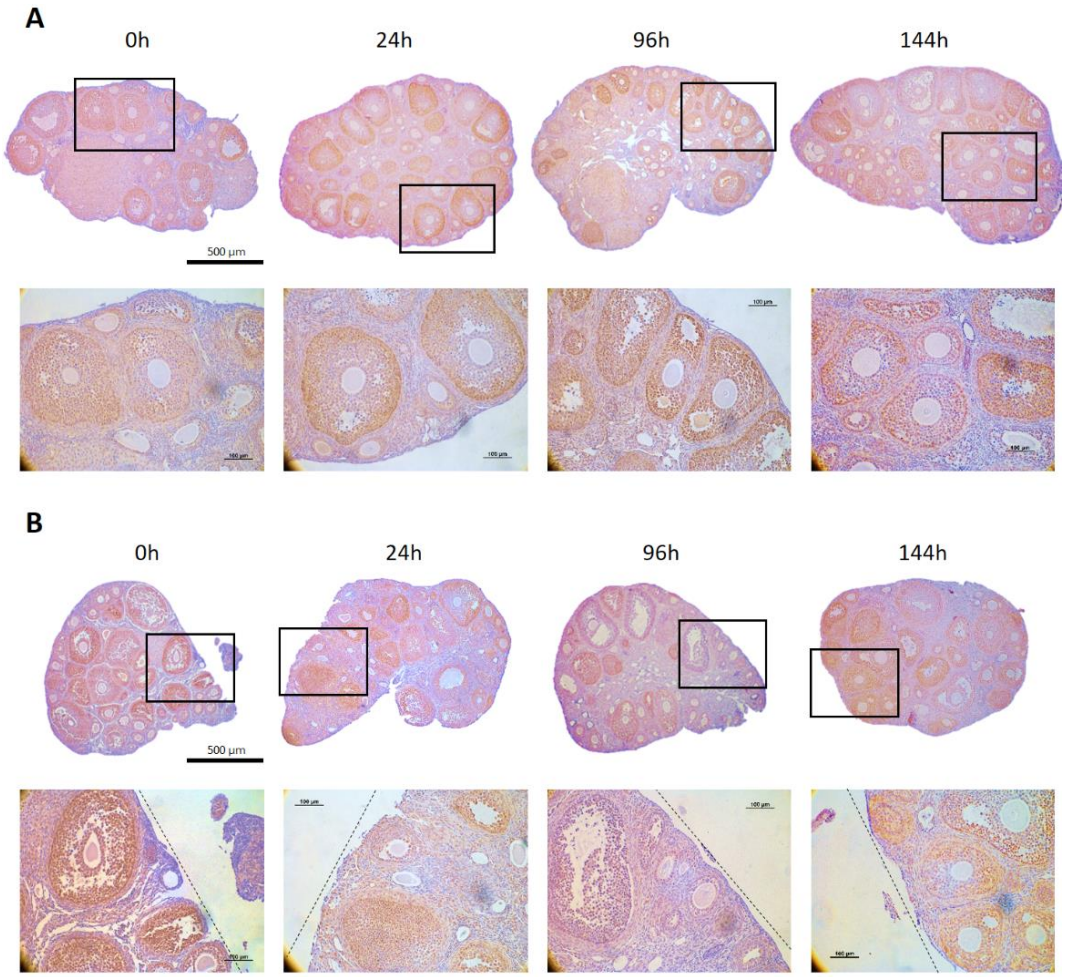

Figure 13. Immunohistochemistry of YAP/TAZ in *Amh* KO mouse ovaries

The expression of YAP/TAZ in *Amh* KO mouse ovaries was histologically compared. (A) Intact ovaries. (B) Cut ovaries. Enlarged details as indicated by the black squares. The scale bar in the enlarged figure represents 100 μm.

p-YAP (ser 127) localization in mouse ovaries

p-YAP was strongly expressed in the granulosa cells of the follicle, but was mainly located in the cytoplasm rather than the nucleus. In wild type ovary, p-YAP showed weak staining compared to 0 h after excision, indicating that the level was decreased (Fig. 14. A, B). In addition, p-YAP was also expressed in the excised part of the ovary. Similarly, in the *Amh* KO ovary, p-YAP was mainly located in the cytoplasm of the granulosa cells (Fig. 15A). After resection, the level of p-YAP decreased at 96 h, but increased at 144 h (Fig. 15B).

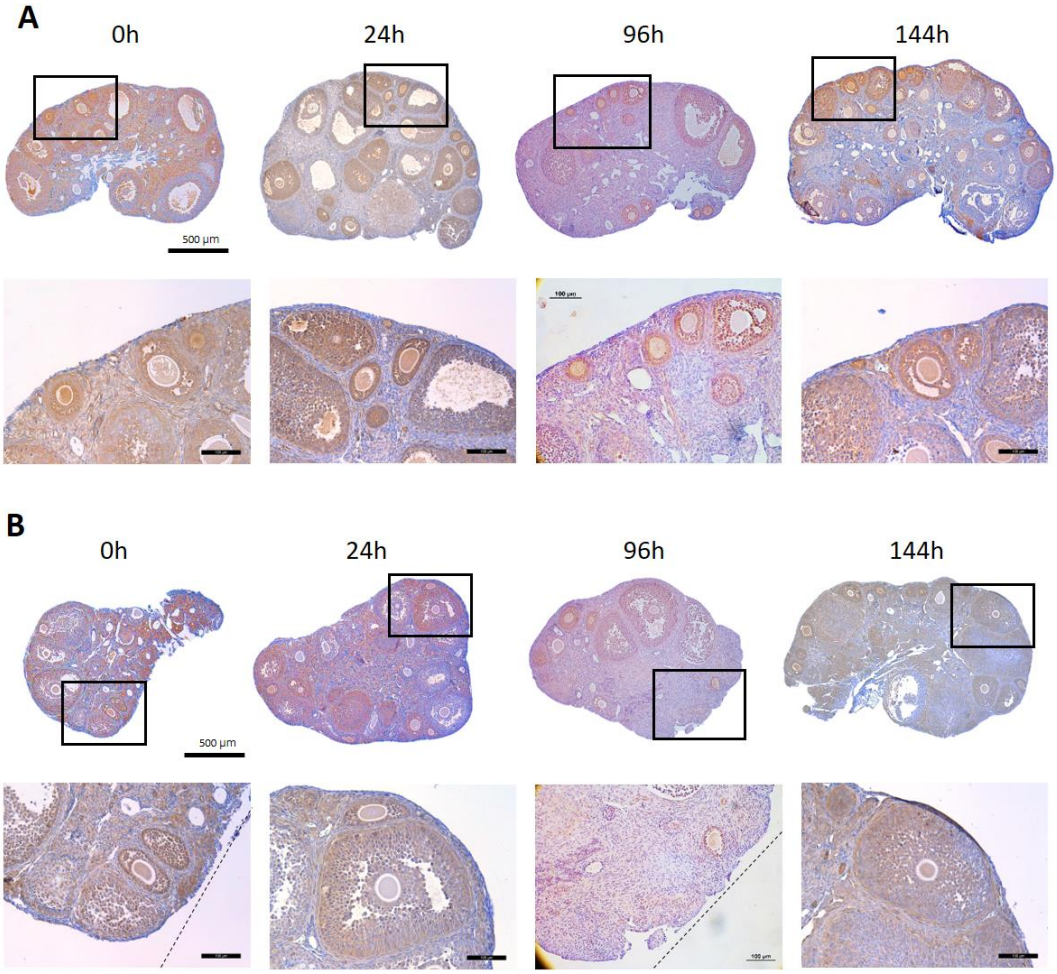

Figure 14. Immunohistochemistry of p-YAP in wild type mouse ovaries

The expression of p-YAP (Ser 127) in wild mouse ovaries was histologically compared. (A) Intact ovaries. (B) Cut ovaries. Enlarged details as indicated by the black squares. The scale bar in the enlarged figure represents 100 μm.

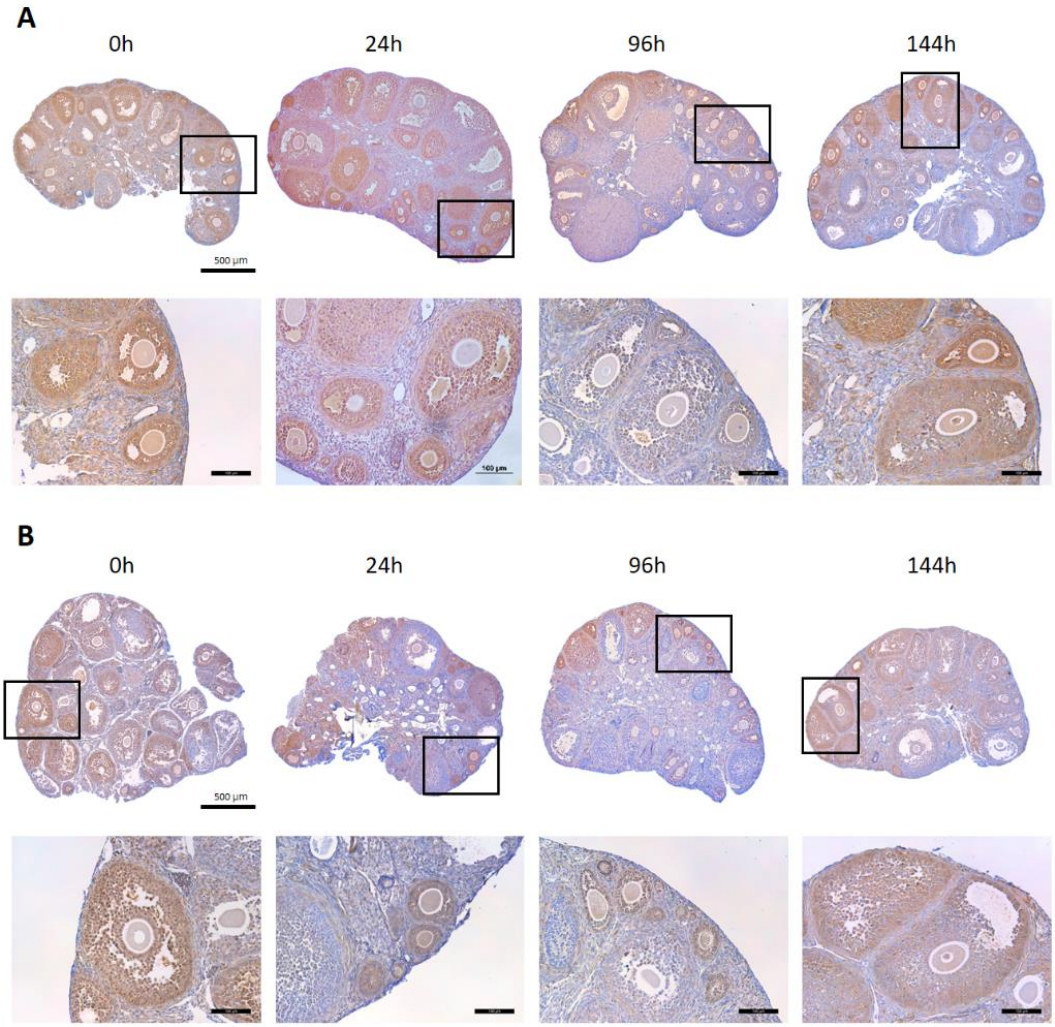

Figure 15. Immunohistochemistry of p-YAP in *Amh* KO mouse ovaries

The expression of p-YAP (Ser 127) in *Amh* KO mouse ovaries was histologically compared. (A) Intact ovaries. (B) Cut ovaries. Enlarged details as indicated by the black squares. The scale bar in the enlarged figure represents 100 μm.

Comparison of the number of follicles in wild-type and anti-Müllerian hormone knockout mice

After ovarian resection, to investigate whether YAP/TAZ activity affects folliculogenesis, the number of ovarian follicles per stage was counted. In wild type ovary, the distribution of primordial follicles in both intact and cut ovaries was predominant, and there was no change in the number of follicles between stages (Fig. 16A, B). 24 h after ovarian resection, primordial follicles in the cut ovary were significantly decreased, and secondary follicles increased. Similarly, at 96 h, primordial follicles decreased significantly, and primary, secondary, and tertiary follicles increased. At 144 h, tertiary follicles increased significantly, and secondary and tertiary follicles showed the most dominant distribution.

In *Amh* KO mice, the secondary follicle was most predominant at 0 h, and there was no significant difference between intact and cut (Fig. 17A, B). After 24 h, the distribution of follicles did not change significantly, but atretic follicles significantly decreased in the cut ovary. Atretic follicle reduction continued up to 144 h. At 96 h, the primary and tertiary follicles increased significantly, and at 144 h, the tertiary follicles increased. Therefore, it can be seen that follicle growth occurred more actively in the ovary from which the part was cut.

The increased YAP/TAZ activity in the ovary promotes folliculogenesis, and the level was relatively small in *Amh* KO mice. Activation of YAP/TAZ resulted in a decrease in atresia in *Amh* KO ovaries. Therefore, these data provide evidence to prove that AMH is involved in Hippo-YAP signaling.

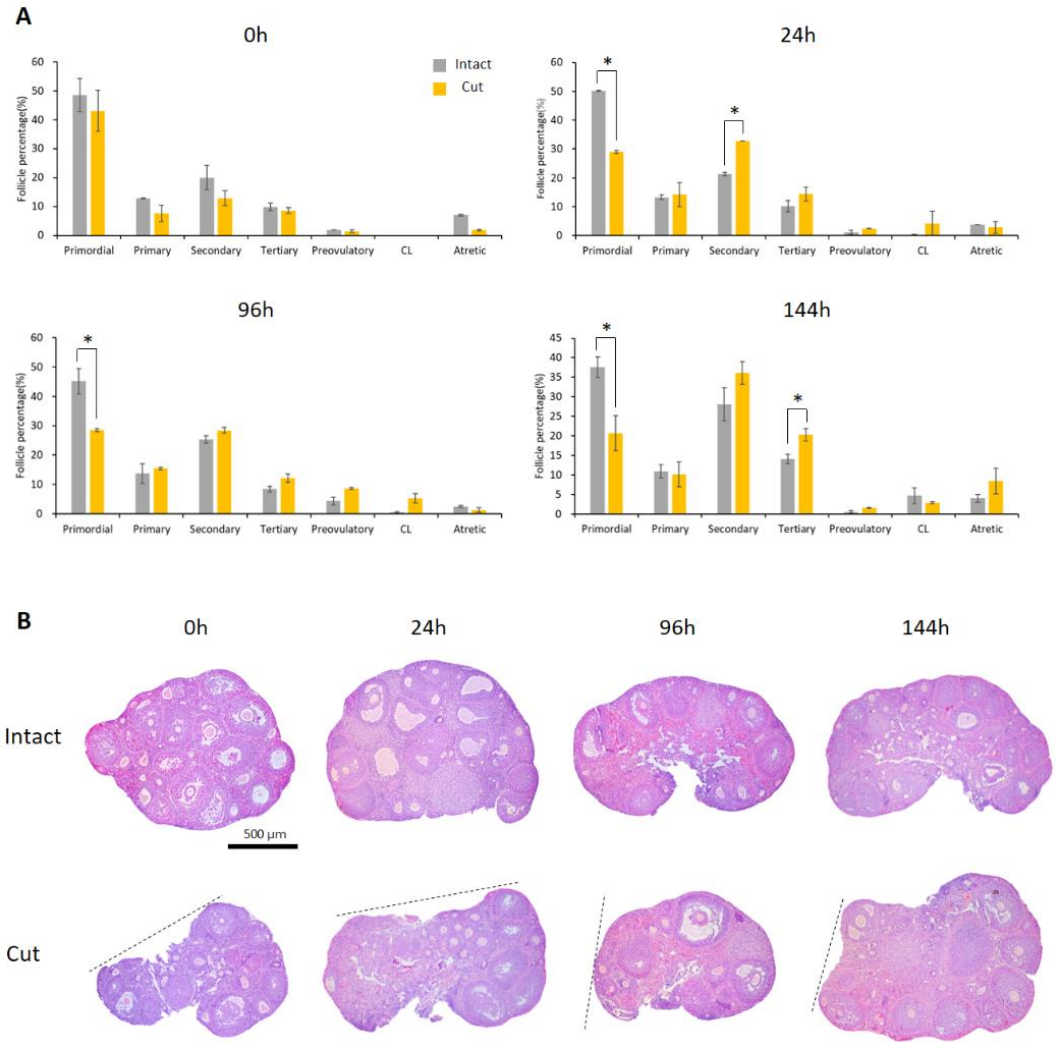

Figure 16. Follicle number comparison in wild type mouse ovaries

The number of follicles was counted by H&E staining on the 10th section of the tissue sectioned to a thickness of 4 μm. (A) Comparison of follicle distribution as a percentage. (B) Histological comparison of ovaries. The dotted line marks the 1/3 cutting site of the ovary.

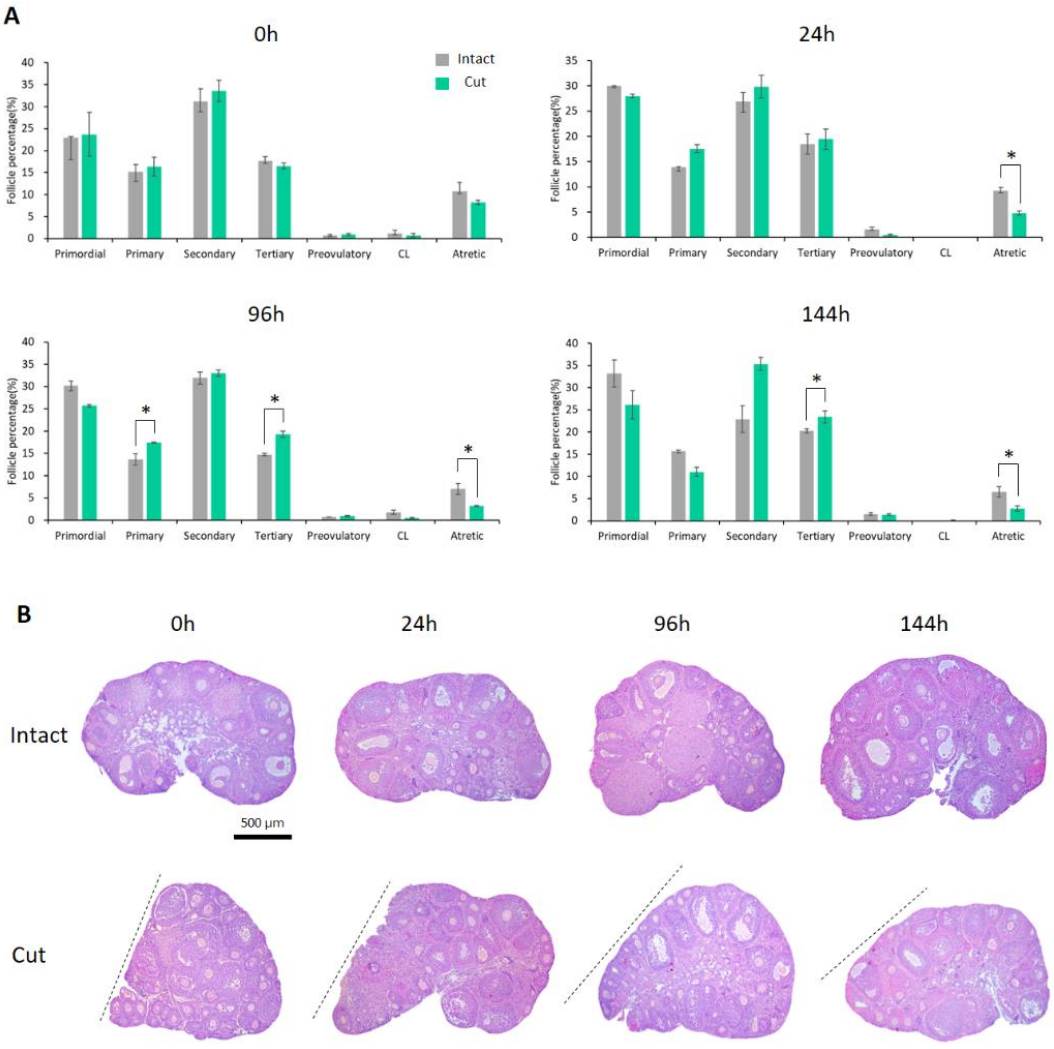

Figure 17. Follicle number comparison in *Amh* KO mouse ovaries

The number of follicles was counted by H&E staining on the 10th section of the tissue sectioned to a thickness of 4 μm. (A) Comparison of follicle distribution as a percentage. (B) Histological comparison of ovaries. The dotted line marks the 1/3 cutting site of the ovary.

DISCUSSION

In this study, YAP/TAZ activity was examined in resected ovaries, and investigated whether folliculogenesis and ovarian weight were changed due to the increase in YAP/TAZ activity. The ovaries from which 1/3 of the total volume were excised significantly increased in weight after 144 h. However, this was not the case in the two-thirds excised ovary. It was confirmed that the activity of YAP/TAZ, which is known as a key effector of the Hippo signaling pathway, was increased in the ovaries showing this change in weight. The expression of YAP/TAZ protein was increased in 1/3 excised ovaries, but not significantly in 2/3 excised ovaries. Based on this fact, 1/3 of the ovaries of *Amh* KO mice were also cut and the changes were compared with those of wild type mice. An increase in the expression of YAP/TAZ was also observed in *Amh* KO mice, but the level was relatively lower than that of wild type. Follicle growth also did not increase as much as wild type.

YAP/TAZ is a key molecule in Hippo signaling pathway and some of the downstream genes have been identified. CTGF is the most well-known target gene for YAP/TAZ and is produced in connective tissue. CTGF has been shown to regulate a diverse array of cellular functions such as angiogenesis, chondrogenesis, and osteogenesis (Arnott et al., 2011). It is also involved in ECM remodeling and epithelial-mesenchymal transition (EMT). In ovaries, CTGF promotes granulosa cell proliferation and has been found to be involved in primordial follicle assembly (Schindler et al., 2010). AREG is a member of the epidermal growth factor (EGF) family. It is a critical autocrine growth factor as well as a mitogen for astrocytes and ligand for EGF. This protein interacts with

the EGF receptor (EGFR) to promote the growth of normal epithelial cells. AREG is a critical factor in estrogen action and ductal development of the mammary glands (Kariagina et al., 2010). In the ovary, AREG induces gene expression required for ECM synthesis and stabilization by cumulus cells (Hsieh et al., 2007). AREG is stimulator of cumulus expansion and promote oocyte maturation. ID1 is a gene whose expression is reduced by YAP/TAZ. ID1 involved in regulating a variety of cellular processes, including differentiation, cellular growth, angiogenesis, senescence and apoptosis. Id1 plays a role in regulating the growth and differentiation of adult ovary steroidogenic cells (Hogg et al., 2010). DDIT4 regulates p53 mediated apoptosis in response to DNA damage via its effect on mTORC1 activity (Tirado-Hurtado et al., 2018). DDIT4 is also a gene that is reduced by YAP/TAZ. The function DDIT4 in the ovary is not defined. The cut ovary of the WT 1/3 group showed increased transcription of *Ctgf* and *Areg* and decreased transcription of *Id1* and *Ddit4* at 144 h after resection along with, highest level of YAP/TAZ. These were suggested that the activity of YAP/TAZ maybe one of the primary regulator of the cell proliferation and has the effect of inhibiting apoptosis.

The ovarian size depends on the population size of the developing follicles. The wet weight was significantly increasd only in 1/3 cutted ovary of wild type. In the follicle population the number of specific follicular stages were different between cutted and control groups in wild type mice. The number of primordial follicles was significantly decreased in cutted group, and the numbers of secondary and tertiary follicles were increased. However, in *Amh* KO mice, the number of primordial follicles was not different between cutted and intact ovary and wet weight. The decrease of the number of primordial follicle and the increase of the secondary and tertiary follicles may the cause of the increase of

ovarian weight in cutted ovary. SMADs are involved in Hippo and *Amh* signaling in cells. Interestingly, the expression of *Smad1* and *Smad2* mRNAs were significantly increased in cutted ovary of wild type but not in *Amh* KO mice. In *Amh* KO mice, the expression level of *Smad2* mRNA was significantly decreased. In addition, the cellular localization of YAP/TAZ was modified in *Amh* KO mice. These results indicated that AMH and Hippo signaling pathway are interconnected.

Put together, these results, reveal AMH can contribute to the activation and inactivation of the Hippo signaling pathway. Furthermore, by interacting with YAP/TAZ, it is suggested the possibility that AMH along with Hippo may play an important role in ovarian size regulation. The evaluate facts, interconnection between AMH and Hippo in folliculogenesis could be useful for the regulation of fertility reservation.

REFERENCES

Arnott JA, Lambi AG, Mundy C, Hendesi H, Pixley RA, Owen TA, Safadi FF, Popoff SN. The role of connective tissue growth factor (CTGF/CCN2) in skeletogenesis. Crit Rev Eukaryot Gene Expr. 2011;21(1):43-69.

Barzegari A, Gueguen V, Omidi Y, Ostadrahimi A, Nouri M, Pavon-Djavid G. The role of Hippo signaling pathway and mechanotransduction in tuning embryoid body formation and differentiation. J Cell Physiol. 2020 Jun;235(6):5072-5083.

Beck TN, Korobeynikov VA, Kudinov AE, Georgopoulos R, Solanki NR, Andrews-Hoke M, Kistner TM, Pépin D, Donahoe PK, Nicolas E, Einarson MB, Zhou Y, Boumber Y, Proia DA, Serebriiskii IG, Golemis EA. Anti-Müllerian Hormone Signaling Regulates Epithelial Plasticity and Chemoresistance in Lung Cancer. Cell Rep. 2016 Jul 19;16(3):657-71.

Cheng Y, Feng Y, Jansson L, Sato Y, Deguchi M, Kawamura K, Hsueh AJ. Actin polymerization-enhancing drugs promote ovarian follicle growth mediated by the Hippo signaling effector YAP. FASEB J. 2015 Jun;29(6):2423-30.

di Clemente N, Josso N, Gouédard L, Belville C. Components of the anti-Müllerian hormone signaling pathway in gonads. Mol Cell Endocrinol. 2003 Dec 15;211(1-2):9-14.

Dunlop CE, Anderson RA. The regulation and assessment of follicular growth. Scand J Clin Lab Invest Suppl. 2014;244:13-7; discussion 17.

Durlinger AL, Kramer P, Karels B, de Jong FH, Uilenbroek JT, Grootegoed JA, Themmen AP. 1999. Control of primordial follicle recruitment by anti-Müllerian hormone in the mouse ovary. Endocrinology. 140(12):5789-96.

Durlinger AL, Visser JA, Themmen AP. Regulation of ovarian function: the role of anti-Müllerian hormone. Reproduction. 2002 Nov;124(5):601-9.

Grosbois J, Demeestere I. Dynamics of PI3K and Hippo signaling pathways during in vitro human follicle activation. Hum Reprod. 2018 Sep 1;33(9):1705-1714.

Gruijters MJ, Visser JA, Durlinger AL, Themmen AP. 2003. Anti-Müllerian hormone and its role in ovarian function. Mol Cell Endocrinol. 211(1-2):85-90.

Hayashi S, Yokoyama H, Tamura K. Roles of Hippo signaling pathway in size control of organ regeneration. Dev Growth Differ. 2015 May;57(4):341-51.

Hayes E, Kushnir V, Ma X, Biswas A, Prizant H, Gleicher N, Sen A. Intra-cellular mechanism of Anti-Müllerian hormone (AMH) in regulation of follicular development. Mol Cell Endocrinol. 2016 Sep 15;433:56-65.

Hogg K, Etherington SL, Young JM, McNeilly AS, Duncan WC. Inhibitor of differentiation (Id) genes are expressed in the steroidogenic cells of the ovine ovary and are differentially regulated by members of the transforming growth factor-beta family. Endocrinology. 2010 Mar;151(3):1247-56.

Hsieh M, Lee D, Panigone S, Horner K, Chen R, Theologis A, Lee DC, Threadgill DW, Conti M. Luteinizing hormone-dependent activation of the epidermal growth factor network is essential for ovulation. Mol Cell Biol. 2007 Mar;27(5):1914-24.

Hu LL, Su T, Luo RC, Zheng YH, Huang J, Zhong ZS, Nie J, Zheng LP. 2019. Hippo pathway functions as a downstream effector of AKT signaling to regulate the activation of primordial follicles in mice. J Cell Physiol. 234(2):1578-1587.

Kariagina A, Xie J, Leipprandt JR, Haslam SZ. Amphiregulin mediates estrogen, progesterone, and EGFR signaling in the normal rat mammary gland and in hormone-dependent rat mammary cancers. Horm Cancer. 2010 Oct;1(5):229-44.

Kastora SL, Triantafyllidou O, Kolovos G, Kastoras A, Sigalos G, Vlahos N. Combinational approach of retrospective clinical evidence and transcriptomics highlight AMH superiority to FSH, as successful ICSI outcome predictor. J Assist Reprod Genet. 2020 Jul;37(7):1623-1635.

Kawamura K, Cheng Y, Suzuki N, Deguchi M, Sato Y, Takae S, Ho CH, Kawamura N, Tamura M, Hashimoto S, Sugishita Y, Morimoto Y, Hosoi Y, Yoshioka N, Ishizuka B, Hsueh AJ. 2013. Hippo signaling disruption and Akt stimulation of ovarian follicles for infertility treatment. Proc Natl Acad Sci USA. 110(43):17474-9.

Kim MK, Jang JW, Bae SC. DNA binding partners of YAP/TAZ. BMB Rep. 2018 Mar;51(3):126-133. doi: 10.5483/bmbrep.2018.51.3.015. PMID: 29366442; PMCID: PMC5882219.

Münsterberg A, Lovell-Badge R. Expression of the mouse anti-müllerian hormone gene suggests a role in both male and female sexual differentiation. Development. 1991 Oct;113(2):613-24.

Lass A, Silye R, Abrams DC, Krausz T, Hovatta O, Margara R, Winston RM. Follicular density in ovarian biopsy of infertile women: a novel method to assess ovarian reserve. Hum Reprod. 1997 May;12(5):1028-31.

Lliberos C, Liew SH, Zareie P, La Gruta NL, Mansell A, Hutt K. Evaluation of inflammation and follicle depletion during ovarian ageing in mice. Sci Rep. 2021 Jan 11;11(1):278.

Lv X, He C, Huang C, Wang H, Hua G, Wang Z, Zhou J, Chen X, Ma B, Timm BK, Maclin V, Dong J, Rueda BR, Davis JS, Wang C. 2019. Timely expression and activation of YAP1 in granulosa cells is essential for ovarian follicle development. FASEB J. 33(9):10049-10064.

Lyu Z, Qin N, Tyasi TL, Zhu H, Liu D, Yuan S, Xu R. The Hippo/MST Pathway Member SAV1 Plays a Suppressive Role in Development of the Prehierarchical Follicles in Hen Ovary. PLoS One. 2016 Aug 9;11(8):e0160896.

Nakamura R, Hiwatashi N, Bing R, Doyle CP, Branski RC. Concurrent YAP/TAZ and SMAD signaling mediate vocal fold fibrosis. Sci Rep. 2021 Jun 29;11(1):13484.

Park JA, Kwon YG. Hippo-YAP/TAZ signaling in angiogenesis. BMB Rep. 2018 Mar;51(3):157-162.

Sacchi S, D'Ippolito G, Sena P, et al. The anti-Müllerian hormone (AMH) acts as a gatekeeper of ovarian steroidogenesis inhibiting the granulosa cell response to both FSH and LH. J Assist Reprod Genet. 2016 Jan; 33(1): 95–100.

Schindler R, Nilsson E, Skinner MK. Induction of ovarian primordial follicle assembly by connective tissue growth factor CTGF. PLoS One. 2010 Sep 24;5(9):e12979.

Sherwood L, Klandorf H, Yancey P. Animal Physiology: From Genes to Organisms. 2004. Brooks Cole.

Stephanie A. Follicular Development: Mouse, Sheep, and Human Models. In: Knobil and Neill's Physiology of Reproduction. 2015. Academic Press. Pp 947-995.

Tirado-Hurtado I, Fajardo W, Pinto JA. DNA Damage Inducible Transcript 4 Gene: The Switch of the Metabolism as Potential Target in Cancer. Front Oncol. 2018 Apr 12;8:106.

Visser JA, Durlinger AL, Peters IJ, van den Heuvel ER, Rose UM, Kramer P, de Jong FH, Themmen AP. Increased oocyte degeneration and follicular atresia during the estrous cycle in anti-Müllerian hormone null mice. Endocrinology. 2007 May;148(5):2301-8.

Visser JA, Themmen AP. Anti-Müllerian hormone and folliculogenesis. Mol Cell Endocrinol. 2005 Apr 29;234(1-2):81-6.

Xiang C, Li J, Hu L, Huang J, Luo T, Zhong Z, Zheng Y, Zheng L. Hippo signaling pathway reveals a spatio-temporal correlation with the size of primordial follicle pool in mice. Cell Physiol Biochem. 2015;35(3):957-68.

논문개요

항-뮐러 호르몬 (AMH) 으로 알려진 뮐러 억제 물질 (MIS) 은 배아 발생 중 성 분화와 난소의 난포 모집에 중요한 요소이다. AMH 는 난포 자극 호르몬 (FSH) 에 대한 민감도를 감소시키고, 원시 난포를 일차 난포로 모집함으로써 FSH 의존성 난포 성장을 억제한다. Hippo 신호전달 경로는 기관의 크기를 조절하는 인자 중 하나로, 최적의 기관 크기를 유지하는 데 필수적이며, 인산화효소 연쇄반응에 작용하는 여러 음성 성장 조절자로 구성된다. Hippo 경로가 활성화되면, MST 1/2 는 LATS 1/2 를 인산화하여 활성화시킨다. 활성화된 LATS1/2 는 Hippo 의 주요 효과자인 전사 조절자 YAP 과 WWTR1 (TAZ) 을 인산화하여 비활성화한다. 반면, Hippo 경로가 비활성화되면, 탈인산화된 YAP/TAZ 가 핵으로 이동하고, TEAD 전사 인자와 결합하여 표적 유전자 전사를 증가시킨다. 증가된 표적 유전자의 발현은 세포 증식, 생존 및 자가 재생을 촉진하며, 세포자멸사를 억제한다. 난소에서 YAP1 의 일시적인 활성화는 난포 성장을 촉진할 수 있으며, LATS1 은 원시 난포 수를 유지하는 역할을 하는 것으로 밝혀졌다. 시험관 내에서 난소의 단편화는 Hippo 를 비활성화하여 YAP 의 핵 전위로 이어지고, 과립막 세포 증식을 촉진하는 표적 유전자 발현을 증가시킨다. AMH 와 Hippo 경로 모두 난포 활성화와 성장에 관여하지만, 현재까지 AMH 와 Hippo 사이의 상호작용에 대한 증거는 부족하다. 본 연구에서는 난소 절제 모델과 *Amh* 유전자 제거 모델을 이용하여 난포형성에서 AMH 와 Hippo 경로의 관계를 조사하였다. *Yap, Taz* 의 발현 변화와, *Ctgf, Areg, Id1* 및 *Ddit4* 의 발현 변화를 조사하고, 조직학적으로 분석하였다. 생쥐 난소를 1/3 절단하자, 난소의 무게는 야생형과 *Amh* 유전자 제거 생쥐 모두에서 시간에 따라 증가했다. *Amh* 유전자 제거 난소에서는 무게 증가가 야생보다 더 느렸다. 절제 후, YAP/TAZ 의 단백질 발현이 유의하게 증가했지만, 그 수준은 야생형보다 *Amh* 유전자 제거 난소에서 더 낮았다. 이와 동시에 부분 절제된 난소에서 2 차 및 3 차 난포의 수가 유의하게 증가했다. 이러한 결과는 AMH 가 Hippo 신호 전달 매개체의 발현과 관련이 있음을 시사한다.